Nuclear Inst. and Methods in Physics Research B 476 (2020) 10–13

Contents lists available at ScienceDirect

Nuclear Inst. and Methods in Physics Research B

journal homepage: www.elsevier.com/locate/nimb

Ion track template technique for fabrication of $ZnSe_2O_5$ nanocrystals

A. Akilbekov[a,*], A. Akylbekova[a], A. Usseinov[a], A. Kozlovskyi[a,b], Z. Baymukhanov[a], Sh. Giniyatova[a], A.I. Popov[c,*], A. Dauletbekova[a,*]

[a] L.N. Gumilyov Eurasian National University, Nur-Sultan, Kazakhstan
[b] Institute of Nuclear Physics, Nur-Sultan, Kazakhstan
[c] Institute of Solid State Physics, University of Latvia, Riga, Latvia

ARTICLE INFO

Keywords:
Ion track
$ZnSe_2O_5$
Track template
Luminescence
Ab initio

ABSTRACT

$ZnSe_2O_5$ nanocrystals with an orthorhombic structure were synthesized by electrochemical deposition into a-SiO_2/n-Si ion track template formed by 200 MeV Xe ion irradiation with the fluence of 10^7 ions/cm^2. The lattice parameters determined by the X-ray diffraction and calculated by the CRYSTAL computer program package are very close to each other. It was shown that $ZnSe_2O_5$ has a direct band gap of 2.8 eV at the Γ-point. In addition, the calculated charge distribution and chemical bonds show that the crystal has an ion-covalent nature. The photoluminescence excited by photons at 300 nm has a low intensity arising mainly due to zinc and oxygen vacancies.

1. Introduction

Ion track technologies are currently a powerful approach for producing new macro- and nanomaterials. From the very beginning, they were based on the idea of using ion tracks [1–4]. Ion tracks and related color centers were observed and studied in detail in a large number of different materials [5–14]. The most striking and impressive application of this technology is associated with the creation of polymer track membranes, the so-called nuclear membranes [15–17]. The current demand and requirements for nuclear membranes are already high and will grow rapidly. Nuclear membranes are obtained by irradiation with heavy ions of a polymer film followed by their physicochemical treatment. As a result, the initial film turns into a microfiltration membrane with through pores of a cylindrical shape. These systems are widely used in physics, medicine and biology [18]. In particular, nuclear membranes with pores measuring 0.5–1 μm in size are widely used for analytical purposes in physicochemical studies as well as in biological and medical experiments, while membranes with pores of diameter 0.1–0.2 μm are used to make filters for fine purification of technological materials in semiconductor device electronics. On the other hand, structures with the smallest pores (< 0.1 μm) are used in the technique of thorough gas processing and in the microbiological industry [15–18]. Note that the controlled formation of pores in technological materials is very important problem for various areas of modern electronics [19–21].

In recent years, using the method of template synthesis, nuclear membranes have been successfully used for the fabrication of various nanomaterials, including, in particular, Ni, Pt, Cu, Ag and Au nanotubes [22] as well as also Ag, Cu, Pt [23], Ni, Ag, Au, Zn and Cu nanoparticles [24–28]. In addition to polymeric materials, a-SiO_2/Si structures have also been frequently and successfully used as ion track templates. Then, using a-SiO_2/Si as a templates, the following structures, such as Au metal nanoclusters [29], Ni and Cu nanoparticles [30], zinc oxide nanocrystals [31,32], or CdTe nanocrystals [9,33] were successfully obtained.

Thus, this method is still promising and successful for the engineering and design of semiconductor materials based on compounds A^3B^5 and A^2B^6 for their integration into silicon technology and possible use for micro-, opto- and nanoelectronics [2,3,16–18].

In this work, using the method of electrochemical deposition on the track template a-SiO_2/n-Si, the formation of zinc diselenide nanocrystals is reported. It can be expected that the synthesized $ZnSe_2O_5$ nanocrystal will not only have properties similar to ZnO and ZnSe, but will also exhibit their own specific and unique characteristics. Therefore, it can be expected that the data obtained will arouse interest in studying the possibility of using $ZnSe_2O_5$ nanocrystals as various active elements in sensors, optoelectronic and nanoelectronic systems that can be currently developed.

2. Experimental

The a-SiO2 / n-Si substrates, in which a is amorphous and n is the

* Corresponding authors.
E-mail addresses: akilbek_ata@mail.ru (A. Akilbekov), popov@latnet.lv (A.I. Popov), alma_dauletbek@mail.ru (A. Dauletbekova).

https://doi.org/10.1016/j.nimb.2020.04.039
Received 1 January 2020; Received in revised form 27 April 2020; Accepted 28 April 2020
Available online 13 May 2020
0168-583X/

type of conductivity, were obtained by thermal oxidation of the (Si-n) disk in a humid oxygen atmosphere at 900 °C with the formation of an oxide layer thickness of 700 nm. Then, samples made with a size of 1x1 cm were irradiated with 200 MeV Xe ions to a fluence of 10^7 ions/cm^2 at a DC-60 cyclotron (Nur-Sultan, Kazakhstan).

Chemical etching of irradiated a-SiO2 / n-Si samples was carried out in a 4% aqueous solution of HF with the addition of palladium (m (Pd) = 0.025 g) at 18° ± 1 °C. Before and after etching of ion tracks, ultrasonic cleaning (6.SB25-12DTS) of the sample surface in isopropanol was carried out for 15 min. After processing, the samples were washed in deionized water (18.2 MΩ). The analysis of nanopores after etching was carried out using a scanning electron microscope (SEM) JSM-7500F.

Electrochemical deposition (ECD) $ZnSe_2O_5$ was carried out, using the following electrolyte: $ZnSO_4 \times 7\ H_2O$–7.2 g/l; SeO_2–0.2 g/l. Firstly, $ZnSO_4$ and SeO_2 were dissolved in deionized water, then two solutions were mixed. For the electrochemical synthesis of nanostructures, a two-electrode cell with zinc cathodes was used, the distance between which is fixed. The process of nanostructure formation in the templates was controlled using the method of chronoamperometry, which consists in controlling the increase in the electric current a a function of time as the pores of the template are filled. Thus the growth of nanostructures was monitored by chronoamperometry using an Agilent 34410A multimeter. The deposition voltage was found to be U = 1.25 V, the voltage that is used to fill the nanopores. X-ray diffraction analysis (XRD) of the samples was carried out on a D8 ADVANCE ECO X-ray diffractometer. The photoluminescence (PL) spectra were recorded, using an Agilent Technologies spectrofluorimeter (Cary Eclipse Fluorescence Spectrophotometer) in spectral range from 300 nm to 800 nm at room temperature at 300 nm excitation.

3. Results and discussion

First of all, ECD was performed on 6 samples that had previously been subjected to ion irradiation. As an example, Fig. 1 shows the SEM images of two samples after ECD. Corresponding analysis of SEM images showed that the number of filled nanopores is on average 80%.

Subsequent X-ray diffraction study of all 6 samples revealed the formation of single-phase $ZnSe_2O_5$ nanocrystals characterized by an orthorhombic crystal structure and belonging to the Pbcn (60) space group, as shown in Table 1.

The lattice parameters obtained above for the orthorhombic unit cell of $ZnSe_2O_5$ are in good agreement with the corresponding data for single crystals [34]. In [35], the preparation of polycrystalline ZnSe films by the chemical deposition (CD) method was made depending on the pH level of the solution, which varied from 8 to 11. In particular, at pH = 11 the simultaneous formation of three phases was found: ZnSe, $ZnSe_2O_5$ and $ZnSeO_3$, while only the two phases ZnSe and $ZnSe_2O_5$ are remained with a pH decrease. It should be noted that there are no detailed reports on $ZnSe_2O_5$, which is clearly related to the difficulty of its preparation in a single-phase state.

To verify the above experimental data for $ZnSe_2O_5$, we also performed *non-empirical* calculations of the $ZnSe_2O_5$ crystal in the approximation of linear combinations of atomic orbitals (LCAO) using the exchange-correlation functional within local density approximation (LDA) [36,37]. The calculations were performed in the CRYSTAL program [38]. This computer program performs calculations of the electronic structure of crystalline systems using the Hartree-Fock methods, density functional (DFT) and various hybrid approximations in combination with the basis set of local (Gaussian) functions for periodic (3D, 2D, 1D) systems and has established itself as a reliable tool to describe the different properties of a wide range of materials.

To describe the atoms of $ZnSe_2O_5$ crystal, the following Gaussian-type basic sets were chosen: the Jaffe basis [39] for the zinc (Zn) and oxygen (O) atoms, and the Towler basis [40] for the selenium (Se) atom. In order to better describe both the structural and electronic properties, the upper *sp*-orbital from original Se basis was removed.

It is known that for a correct description of the electronic structure of a crystal, it is necessary to accurately determine the total energy of the crystal cell [41,42]. In CRYSTAL calculations high convergence tolerances for the Coulomb and exchange integrals have been chosen for the Coulomb overlap (10^{-7}), Coulomb penetration (10^{-7}), exchange overlap (10^{-7}), first exchange pseudo overlap (10^{-7}), and the second exchange pseudo overlap (10^{-14}). The effective atomic charges were calculated using the Mulliken analysis [43].

We have used a periodic supercell model of a primitive $ZnSe_2O_5$

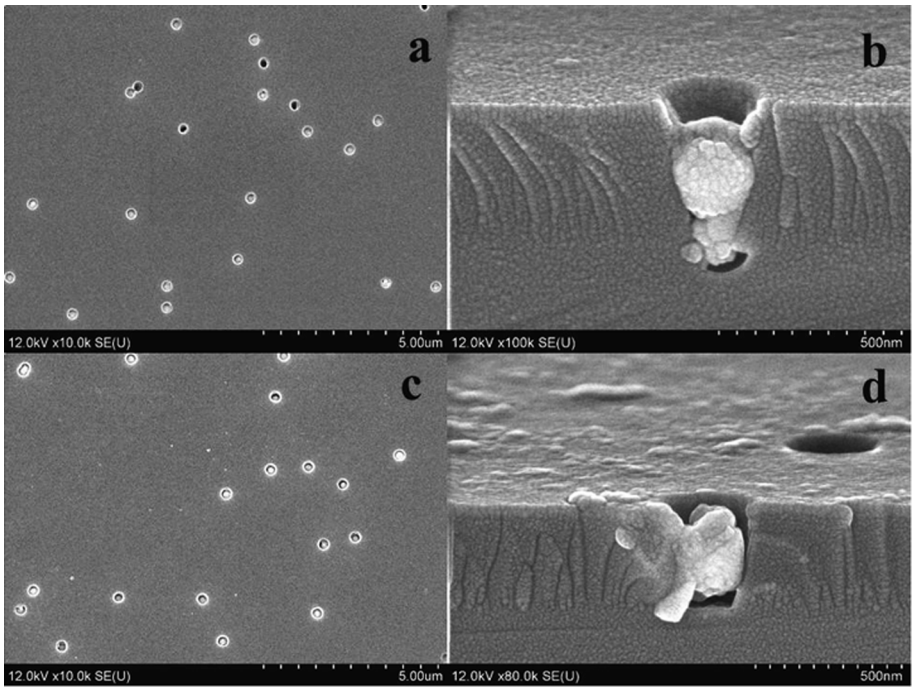

Fig. 1. SEM images of the surface and the transverse cleavage of two samples deposited at 1.25 V (a, c — surfaces, b, d — cross section).

Table 1
Parameters of $ZnSe_2O_5$ nanocrystals.

№	Phase	Structure type	Space group	(*hkl*)	2θ°	d, Å	Cell parameters, Å	Degree of crystallinity %
1	$ZnSe_2O_5$	Orthorhombic	Pbcn(60)	113 161	47.669 56.573	1.90623 1.62550	a = 6.84898, b = 10.40588 c = 6.10726	60
2	$ZnSe_2O_5$	Orthorhombic	Pbcn(60)	222 161	43.532 56.668	2.07729 1.62301	a = 6.82438, b = 10.30182 c = 6.08451	62
3	$ZnSe_2O_5$	Orthorhombic	Pbcn(60)	161	56.605	1.62467	a = 6.83702, b = 10.34424 c = 6.10479	65,1
4	$ZnSe_2O_5$	Orthorhombic	Pbcn(60)	161	56.668	1.62301	a = 6.82495, b = 10.30976 c = 6.16404	62
5	$ZnSe_2O_5$	Orthorhombic	Pbcn(60)	222 115 161	43.596 47.985 56.637	2.07442 1.89442 1.62384	a = 6.77276, b = 10.41286 c = 6.18404	76
6	$ZnSe_2O_5$	Orthorhombic	Pbcn(60)	222 161	43.564 56.637	2.07585 1.62384	a = 6.71034, b = 10.34140 c = 6.24588	58,6

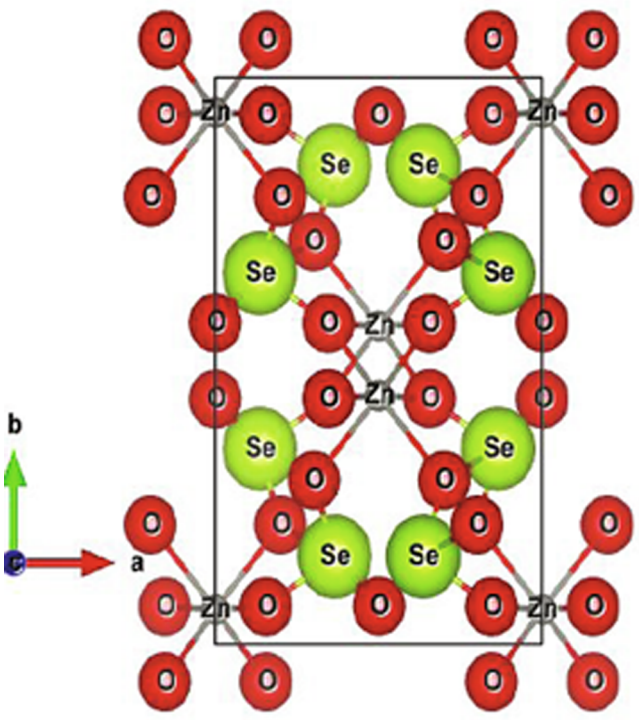

Fig. 2. Atomic structure of $ZnSe_2O_5$ unit cell (32 atoms). The boundaries of the cell and the directions of the translation vectors are shown.

Table 2
Calculated parameters of $ZnSe_2O_5$ crystal.

Parameter	This work, (calculations)	This work, (experiment)	[34] (experiment)
a, Å	6.86	6,71034 Å	6.797 ± 0.002 Å
b, Å	10.14	10,34140 Å	10.412 ± 0.003 Å
c, Å	5.77	6,24588 Å	6.068 ± 0.002 Å
Space group	*Pbcn*	*Pbcn*	*Pbcn*
ρ_V (g/cm^3)	4.971	–	4.44
q_{eff} (Zn/Se/O)	+1.23/+1.41/−0.833	–	–

cell, consisting of 32 atoms (Fig. 2). The calculated lattice parameters (*a*, *b*, *c*), crystal density (ρ_V), and effective atomic charges (q_{eff}) are presented in Table 2 together with experimental results.

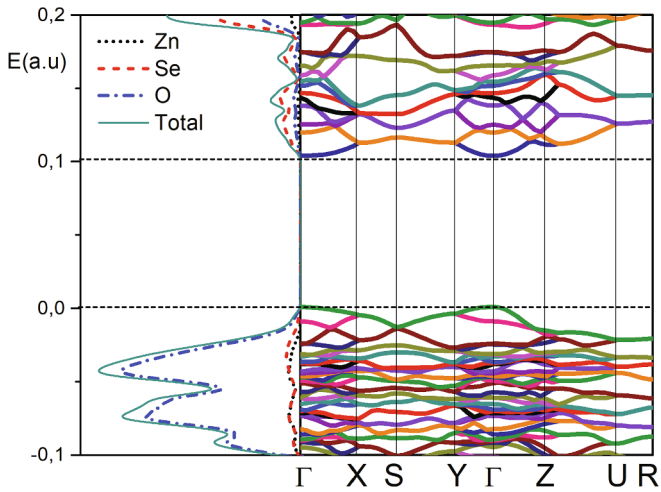

Fig. 3. Density of states and band structure of pure $ZnSe_2O_5$ crystal. The horizontal dashed lines indicate the limits of the valence and conduction bands.

Fig. 3 shows the band structure of the crystal together with the density of the electronic states (DOS). As follows from the Fig. 3, the bandgap energy of $ZnSe_2O_5$ is 2.8 eV (which is close to earlier calculated value of 3.04 eV [44]) and that the band gap is direct at the Γ point of the Brillouin zone. In addition, as clearly seen from DOS, the valence band is represented mainly by O 2p orbitals, while the conduction band mainly consists of Zn 3d, 4s and Se 3d, 4s orbitals, which indicates at essentially ionic compound. However, charge distribution analysis shows also significant covalent contribution to the Se-O chemical bonding in the crystal.

Finally, we performed test measurements of the luminescent properties of $ZnSe_2O_5$, which can be expected as a symbiosis of the luminescence of both zinc oxide and zinc selenide. From the luminescent point of view, a qualitative analysis of the structure of $ZnSe_2O_5$ (Fig. 2) shows that in its luminescence, the contribution due to ZnO should be more predominant than the contribution from the luminescence of ZnSe, since, as follows from the crystal structure of $ZnSe_2O_5$, the Zn-Se bond is realized through O.

Fig. 4 shows the differential PL spectrum after ECD, which displays all the common features for all 6 deposited samples. A comparison of this spectrum with the PL spectra of ZnO [45–48] and ZnSe [49] allows us to assume that the PL band with a maximum of 500 nm (2.48 eV) (green luminescence) can be due to oxygen vacancies (V_O) as in ZnO

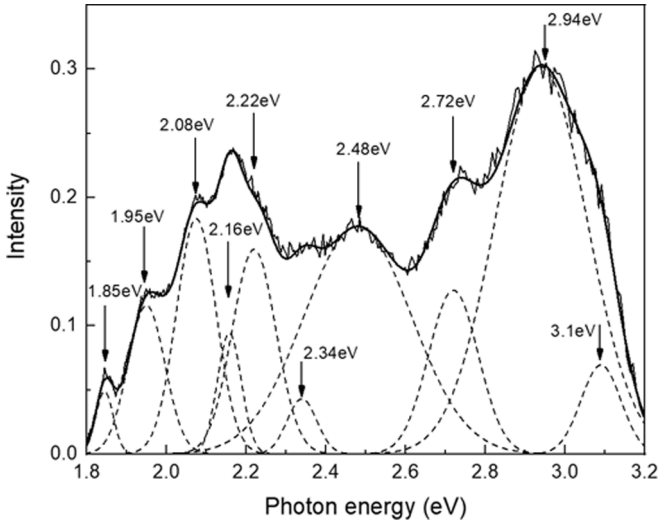

Fig. 4. Differential PL spectra after ECD of $ZnSe_2O_5$.

[43], while the band with a maximum of 422 nm (2.94 eV) (blue luminescence), is due to zinc vacancies (V_{Zn}) [43] in ZnO. Thus, the PL band with a maximum of 422 nm can be associated with zinc vacancies (V_{Zn}) in the $ZnSe_2O_5$ lattice. In the X-ray and photoluminescence spectra of ZnSe single crystals, wide recombination bands with peaks at 626 and 963 nm have been observed [44]. In our case, the PL band has also a maximum at 635 nm (1.95 eV). In the case ZnSe, similar feature has been assigned to a complex center consisting of a zinc vacancy and an impurity small donor V_{Zn} + D [49].

For a detailed interpretation of the photoluminescence spectra, it is necessary to carry out detailed measurements and analysis of the corresponding luminescence excitation spectra, which will be the subject of further research.

4. Conclusions

The $ZnSe_2O_5$ nanocrystals obtained by the method of electrochemical deposition into a 200 MeV Xe ion track template (a-SiO_2/n-Si) have an orthorhombic crystal structure and crystal lattice parameters coinciding with those for the single crystals. In addition, using the CRYSTAL computer program package, the $ZnSe_2O_5$ lattice parameters were also calculated, which were found to be almost close to experimental ones. It was also shown that $ZnSe_2O_5$ reveals the direct-band gap of 2.8 eV at the Γ-point. In addition, the calculated charge distribution and chemical bonds show that the crystal has an ion-covalent nature. The PL excited by light at 300 nm showed a low intensity and is mainly due to zinc and oxygen vacancies.

Declaration of Competing Interest

The authors declare that they have no known competing financial interests or personal relationships that could have appeared to influence the work reported in this paper.

Acknowledgements

The work was performed under the grant of the Ministry of Education and Science of the Republic of Kazakhstan AP05134367, while AIP was supported by Institute of Solid State Physics, University of Latvia via Latvian project lzp-2018/1-0214.

References

[1] D. Fink, L.T. Chadderton, K. Hoppe, W.R. Fahrner, A. Chandra, A. Kiv, Nucl. Instr. Meth. B 261 (2007) 727.
[2] D. Fink, A. Petrov, H. Hoppe, W.R. Fahrner, R.M. Papaleo, A. Berdinsky, A. Chandra, A. Biswas, L.T. Chadderton, Nucl. Instr. Meth. B 218 (2004) 355.
[3] D. Fink, A. Petrov, W.R. Fahrner, K. Hoppe, R.M. Papaleo, A. Berdinsky, A. Chandra, A. Zrineh, L.T. Chadderton, Int. J. Nanosci 4 (2005) 965.
[4] K. Hoppe, W.R. Fahrner, D. Fink, S. Dhamodoran, A. Petrov, A. Chandra, A. Saad, F. Faupel, V.S.K. Chakravadhanula, V. Zaporotchenko, Nucl. Instr. Meth. B 266 (2008) 1642.
[5] A. Dauletbekova, K. Schwartz, M.V. Sorokin, A. Russakova, M. Baizhumanov, A. Akilbekov, M. Zdorovets, M. Koloberdin, Nucl. Instr. Meth. B 326 (2014) 311.
[6] A. Dauletbekova, K. Schwartz, M.V. Sorokin, J. Maniks, A. Rusakova, M. Koloberdin, A. Akilbekov, M. Zdorovets, Nucl. Instr. Meth. B 295 (2013) 89.
[7] M.L. Crespillo, F. Agulló-López, A. Zucchiatti, Nucl. Instr. Meth. B 394 (2017) 20.
[8] K. Kimura, S. Sharma, A.I. Popov, Nucl. Instrum. Meth. B, 191 (2002) 48; Radiation Measurements, 34 (2001) 99.
[9] R. Balakhaeva, A. Akylbekov, A. Dauletbekova, A. Kozlovsky, Z. Baymukhanov, Sh. Giniyatova, A. Useinov, AIP Conf. Proc. 2174 (2019) 020006.
[10] A.J. van Vuuren, M.M. Saifulin, V.A. Skuratov, J.H. O'Connell, G. Aralbayeva, A. Dauletbekova, M. Zdorovets, Nucl. Instr. Meth. B 460 (2019) 67.
[11] G. Szenes, F. Paszti, A. Peter, A.I. Popov, Nucl. Instr. Meth. B 166–167 (2000) 949.
[12] A. Popov, E. Balanzat, Nucl. Instr. Meth. B 166 (2000) 545.
[13] D.V. Ananchenko, S.V. Nikiforov, V.N. Kuzovkov, A.I. Popov, G.R. Ramazanova, R.I. Batalov, R.M. Bayazitov, H.A. Novikov, Nuclear Inst. Meth. B 466 (2020) 1–7.
[14] R.S. Averback, P. Ehrhart, A.I. Popov, A. von Sambeek, Radiation Effects Defects Solids 136 (1995) 169.
[15] P.Y. Apel, Track-Etching. Encyclopedia of Membrane Science and Technology, Wiley, 2013, p. 25.
[16] P. Apel, Radiation Measurements 34 (2001) 559–566.
[17] G.N. Flerov, P.Y. Apel, A.Y. Didyk, V.I. Kuznetsov, R.T. Oganesyan, Soviet Atomic Energy 67 (1989) 763–770.
[18] M.V. Hoek, V.V. Tarabara (Eds.), Track-Etching. Encyclopedia of Membrane Science and Technology, Part IV. Membrane Applications, Wiley, 2013, p. 2390.
[19] J.A. Suchikova, J. Nano- Electron. Phys. 7 (2015) 03017.
[20] Y.A. Suchikova, V.V. Kidalov, G.A. Sukach, J. Nano- Electron. Phys. 1 (4) (2009) 78–86.
[21] Y.O. Suchikova, J. Nano- Electron. Phys. 9 (2017) 01006.
[22] L. Velleman, J.G. Shapter, D. Losic, J. Membr. Sci. 328 (2009) 121.
[23] F. Muench, M. Oezaslan, T. Seidl, S. Lauterbach, P. Strasser, H.-J. Kleebe, W. Ensinger, Appl. Phys. A 105 (2011) 847.
[24] I. Enculescu, M. Sima, M. Enculescu, E. Matei, M.E. Toimil Molares, Th Cornelius, Optoelectron. Adv. Mat. 2 (2008) 133.
[25] P. Shao, J. Membr. Sci. 255 (2005) 1.
[26] V. Kumar, R. Singh, S.K. Chakarvarti, Dig. J. Nanomater. Biostruct. 2 (2007) 163.
[27] M. Pashchanka, R.C. Hoffmann, A. Gurlo, J.C. Swarbrick, J. Khanderi, J. Engstler, A. Issanin, J.J. Schneider, Dalton Trans. 40 (2011) 4307.
[28] D.B. Kadyrzhanov, M.V. Zdorovets, A.L. Kozlovskiy, L.E. Kenzhina, A.V. Petrov, Mater. Res. Express. 4 (2017) 125023.
[29] P. Kluth, B. Johannessena, C.J. Glover, M.C. Foran, Ridgway. Nucl. Instr. Meth. B. 238 (2005) 285.
[30] Yu.A. Ivanova, D.K. Ivanou, A.K. Fedotov, E.A. Streltsov, S.E. Demyanov, A.V. Petrov, E.Yu. Kaniukov, J Mater Sci. 42 (2007) 9163.
[31] A. Dauletbekova, L. Vlasukova, Z. Baimukhanov, A. Akilbekov, A. Kozlovskiy, Sh. Giniyatova, A. Seitbayev, A. Usseinov, A. Akylbekova, Phys. Stat. Sol. B 256 (2019) 1800408.
[32] Sh. Giniyatova, A. Dauletbekova, Z. Baimukhanov, L. Vlasukova, A. Akilbekov, A. Usseinov, A. Kozlovskiy, A. Akylbekova, Radiation Measurements 125 (2019) 52.
[33] D.K. Ivanou, E.A. Streltsov, A.K. Fedotov, A.V. Mazanik, D. Fink, A. Petrov, Thin Solid Films 490 (2005) 154.
[34] G. Meunier, M. Bertaud, Acta Crystallographica. Section B 30 (1974) 2840.
[35] F.M. Tezel, İ.A. Kariper, Int. J. Modern Phys. B 33 (2019) 1950024.
[36] P.A.M. Dirac, Proc. Cambridge Phil. Soc. (1930) 376.
[37] J.P. Perdew, A. Zunger, Phys. Rev. B (1981) 5048.
[38] R. Dovesi, V.R. Saunders, R. Roetti, R. Orlando, C.M. Zicovich-Wilson, F. Pascale, B. Civalleri, K. Doll, N.M. Harrison, I.J. Bush, P. D'Arco, M. Llunell. CRYSTAL14 User's Manual University of Torino, Torino (2014).
[39] J.E. Jaffe, A.C. Hess, Phys. Rev. B 48 (1993) 7903.
[40] Selenium basis set for Crystal Program, (http://www.tcm.phy.cam.ac.uk/~mdt26/basis_sets/Se_basis.txt).
[41] F. Gallino, G. Pacchioni, C. Di Valentin, J. Chem. Phys. 133 (2010) 144512.
[42] C.G. Van de Walle, J. Neugebauer, Appl. Phys. Lett. 95 (2008) 3851.
[43] R.S. Mulliken, J. Chem, Phys. 23 (1955) 1833.
[44] A. Jain, S.P. Ong, G. Hautier, W. Chen, W.D. Richards, S. Dacek, S. Sholia, D. Gunter, D. Skinner, G. Ceder, K.A. Persson, APL Materials 1 (2013) 011002.
[45] A.V. Uklein, V.V. Multian, G.M. Kuz'micheva, R.P. Linnik, V.V. Lisnyak, A.I. Popov, V.Ya. Gayvoronsky, Opt. Mater. 84 (2018) 738.
[46] B. El Filali, J.A. Jaramillo Gomez, T.V. Torchynska, J.L. Casas Espinola, L. Shcherbyna, Opt. Mater 89 (2019) 322.
[47] S.A. Studenikin, N. Golego, M. Cocivera, J. Appl. Phys. 84 (1998) 2287.
[48] H. Kumano, A.A. Ashrafi, A. Ueta, A. Avramescu, I. Suemune, J. Cryst. Growth 214 (215) (2000) 280.
[49] V.Ya. Degoda, A.O. Sofienko, Semiconductors 44 (2010) 1.